1P1-3

Measurement of Locally Resonant Band Gaps in a Surface Phononic Crystal with Inverted Conical Pillars

Jin-Chen Hsu[1†] and Fan-Shun Lin[1] ([1]Department of Mechanical Eng., National Yunlin Univ. of Sci. and Tech)

1. Introduction

Phononic crystals (PnCs) are heterogeneous materials that exhibit periodic modulation of their mass density and elastic properties. With PnCs, the propagation behaviors of elastic/acoustic waves can be tailored and manipulated [1]. During the past few years, surface PnCs, where mass density and elastic properties are modulated along the surface of a semi-infinite substrate, have received increasing attention, as its fundamental functionality can be tailored to manipulate the surface acoustic waves (SAWs) [2]. One of the most interesting features is the existence of acoustic band gaps, in which the propagation of SAWs is prohibited in some specific frequency ranges. This phenomenon can be used for broad applications with different frequency ranges and characteristic dimensions, including frequency filtering, and sound and vibration isolation.

Surface PnCs provide mechanisms to support more surface mode branches in the band structures and leaky surface modes above the sound cone of the substrate. The mechanisms arise from the fact that the modulated surface can trap and couple the acoustic waves of different modes (e.g., resonant modes of the surface PnC scatterers and bulk modes of the substrate). Recently, many researchers have conducted studies on surface PnCs with surfaces structured by one-dimensional or two-dimensional arrays of pillars, holes, or resonators [3,4]. Several studies have reported that shaping the pillars to tune the resonant responses (e.g., stiffness and mass) can be applied to modulate the frequency range of the local resonance (LR) and band gaps for thin-plate modes [5,6]. However, the effect has rarely been discussed experimentally on the micrometer scale surface PnCs for SAW modes.

In the present study, we present the numerical and experimental results of the LR band gaps in 2D surface PnCs by fabricating honeycomb arrays of inverted conical nickel pillars on a 128°YX $LiNbO_3$ substrate. Compared to cylindrical pillars, the use of inverted conical pillars can produce an observable effect on decreasing the LR band-gap frequencies.

2. Methods

Figure 1 shows the schematics of the surface PnC with inverted conical pillars and its unit cell.

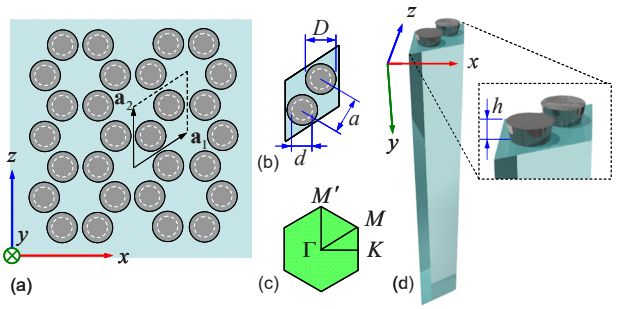

Fig. 1 (a) Schematic of the honeycomb pillar array viewed on the *x*-*z* plane. (b) Definition of the unit cell . (c) The corresponding first BZ. (d) 3D geometry of the unit-cell model.

The inverted conical pillars are deposited on a semi-infinite $LiNbO_3$ substrate and arranged in a honeycomb lattice array. We assume the inverted conical pillars have a larger top diameter D, smaller bottom diameter d, and height h. Thus, the inverted conical pillars have more mass distributed around the top and from their attached bottom. The lattice constant here is assumed to be a. Calculations of the band structures were performed using the finite element method with periodic boundary conditions. We determine the band gaps below the sound cone with a variable bandwidth for the SAW modes by changing the pillar dimensions.

In the experiment, we fabricated honeycomb surface PnC consisting of inverted conical pillars of h = 3.0 μm, d = 6.4 μm, and D = 7.6 μm arranged with a = 10 μm. The pillar array was deposited on a $LiNbO_3$ wafer of 500-μm thickness. A set of SFITs are placed on both sides of an inverted conical pillar array. The left SFIT generated wideband Rayleigh SAWs to impinge on the honeycomb array, and the right SFIT received the electrical response of the transmitted SAWs by means of piezoelectric effect provided by the $LiNbO_3$ substrate. The electrical transmission measurements are performed using a network analyzer (Agilent N5245A). To cover the frequency range of interest, three different SFIT designs were employed.

3. Results and Discussion

Initially, we consider the straight cylindrical pillars with a fixed height h = 3.0 μm. It has been reported that the frequency location of the SAW LR band gaps of cylindrical pillar-based surface PnCs are dominated by the pillar height. **Figures 2(a)** and

† Email: hsujc@yuntech.edu.tw

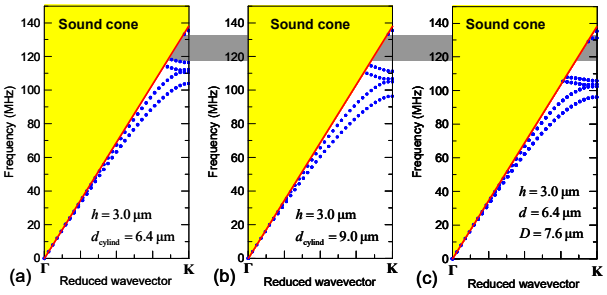

Fig. 2 Calculated band structures along the Γ*K* direction of the first BZ for the surface PnC with (a, b) cylindrical and (c) inverted conical pillars.

2(b) present the frequency band structures along the Γ*K* direction of the first Brillouin zone (BZ) for the 2D surface PnC with cylindrical pillars of different diameters d_{cylind}. The lattice constant is a = 10 μm. The result displayed in Fig. 2(a) corresponds to the use of cylindrical pillars with d_{cylind} = 6.4 μm, where a SAW LR band gap is generated and ranges from 119 to 133 MHz below the sound cone. In Fig. 2(b), when the diameters are as large as d_{cylind} = 9.0 μm, the lower band-gap frequency slightly decreases to 115 MHz. In **Fig. 2(c)**, we consider that the pillars have a bottom diameter d = 6.4 μm, top diameter D = 7.6 μm, and height h = 3.0 μm. The first SAW LR band gap range is lowered to 108–129 MHz below the sound cone. Compared with Figs. 2(a) and 2(b), the use of inverted conical pillar array can be more effective at shifting down the SAW LR band gap than using cylindrical pillar array at the same pillar height. The result can be understood by the fact that using inverted conical pillars is more effective at increasing the resonant mass without increasing the contact area with the substrate. As a result, the locally resonant frequency can be further decreased. Leaving the bottom diameter of the inverted conical pillars unchanged.

The measured electrical transmission signals

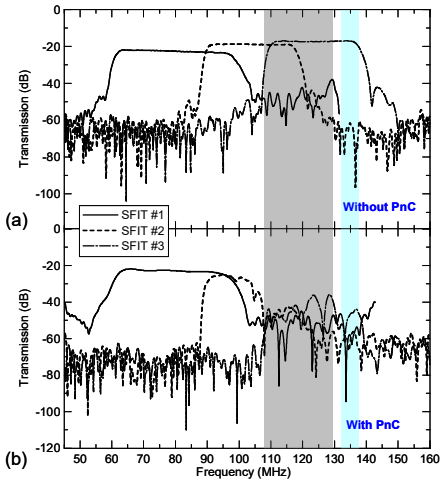

Fig. 3 Measured electrical transmission signals (a) without and (b) with the surface PnC.

are shown in **Fig. 3**. Figure 3(a) displays that the transmissions are in the absence of pillar array. The signals characterize the responses of the devices, as given by Rayleigh SAWs propagating freely on the surface of the $LiNbO_3$ substrate, and serve as a reference. The SAW bandwidths of the three sets of SFITs successfully extend from 60–100, 90–120, and 110–140 MHz, respectively, with a dynamic range in excess of 30 dB. In the figure, the gray shadow region denotes the claculated LR band gap for SAWs. The three measured transmission signals for SAWs through the honeycomb surface PnC are shown in Fig. 3(b). Along the propagation direction, the measured structure contains twelve periods of honeycomb-lattice pillar arrays. As we examine the transmissions of the measured frequency ranges, the signal intensity with the inverted conical pillar array is similar to the intensity of the reference signal for frequencies ranging from 60 to 105 MHz. A drastic drop in transmission signal intensity occurs around 108 MHz. For frequencies up to 140 MHz, however, the transmission signal has an extinction ratio of about 20 dB because of approaching the sound cone. The measured frequency range of the band gap is in good agreement with the numerical results that the inverted conical pillars induced a lower LR band gap for SAWs.

4. Conclusions

We have numerically and experimentally studied the lowering of an LR band gap for SAWs using inverted conical pillars. This lowering effect is primarily due to the increase in the effective mass without increasing the effective stiffness of the pillar resonators such that the LR frequency can be decreased. The measured band-gap frequency range is in good agreement with the numerical prediction. The observation suggests an alternative to tune LR frequencies by pillar shapes at the micrometer scale instead of increasing the pillar height.

Acknowledgment

This work was supported by MOST, Taiwan. Grant Number: MOST 103-2221-E-224-002-MY3

References

1. M. I. Hussein, M. J. Leamy, and M. Ruzzene: Appl. Mech. Rev. **66** (2014) 040802.
2. T.-W. Liu, Y.-C. Lin, Y. C. Tsai, T. Ono, S. Tanaka, and T.-T. Wu: Appl. Phys. Lett. 104 (2014), 181905.
3. Y. Achaoui, V. Laude, S. Benchabane, and A. Khelif: J. Appl. Phys. **114** (2013) 104503.
4. M. B. Assouar, J.-H. Sun, F.-S. Lin, and J.-C. Hsu: Ultrasonics **54** (2014) 2159.
5. J-.C. Hsu: Jpn. J. Appl. Phys. **51**, 07GA04.
6. J-.C. Hsu: J. Phys. D **44** (2011) 055401.